\$ SEVIER

Contents lists available at ScienceDirect

Acta Biomaterialia

journal homepage: www.elsevier.com/locate/actbio



Full length article

The flying insect thoracic cuticle is heterogenous in structure and in thickness-dependent modulus gradation



Cailin Casey^a, Claire Yager^b, Mark Jankauski^{a,*}, Chelsea M. Heveran^{a,*}

- ^a Mechanical and Industrial Engineering, Montana State University, 220 Roberts Hall Bozeman, MT 59717, United States
- ^b Ecology, Montana State University, 310 Lewis Hall Bozeman, MT 59717, United States

ARTICLE INFO

Article history: Received 30 June 2021 Revised 20 October 2021 Accepted 21 October 2021 Available online 3 November 2021

Keywords: Insect flight Thorax Cuticle Nanoindentation Modulus gradation

ABSTRACT

The thorax is a specialized structure central to insect flight. In the thorax, flight muscles are surrounded by a thin layer of cuticle. The structure, composition, and material properties of this chitinous structure may influence the efficiency of the thorax in flight. However, these properties, as well as their variation throughout the thorax and between insect taxa, are not known. We provide a multi-faceted assessment of thorax cuticle for fliers with asynchronous (honey bee; Apis mellifera) and synchronous (hawkmoth; Manduca sexta) muscles. These muscle types are defined by the relationship between their activation frequency and the insect's wingbeat frequency. We investigated cuticle structure using histology, resilin distribution through confocal laser scanning microscopy, and modulus gradation with nanoindentation. Our results suggest that thorax cuticle properties are highly dependent on anatomical region and species. Modulus gradation, but not mean modulus, differed between the two types of fliers. In some regions, A. mellifera had a positive linear modulus gradient from cuticle interior to exterior of about 2 GPa. In M. sexta, modulus values through cuticle thickness were not well represented by linear fits. We utilized finite element modeling to assess how measured modulus gradients influenced maximum stress in cuticle. Stress was reduced when cuticle with a linear gradient was compressed from the high modulus side. These results support the protective role of the A. mellifera thorax cuticle. Our multi-faceted assessment advances our understanding of thorax cuticle structural and material heterogeneity and the potential benefits of material gradation to flying insects.

Statement of significance

The insect thorax is essential for efficient flight but questions remain about the contribution of the exoskeletal cuticle. We investigated the microscale properties of the thorax cuticle, a crucial step to determine its role in flight. Techniques including histology, nanoindentation, and confocal laser scanning microscopy revealed that cuticle properties vary through cuticle thickness, by thorax region, and between species with asynchronous (honey bee; *Apis mellifera*) and synchronous (hawkmoth; *Manduca sexta*) muscles. This variation highlights the importance of high resolution cuticle assessment for flying insect lineages and points to factors that may (modulus gradation) and may not (mean modulus) contribute to different flight forms. Understanding material variation in the thorax may inform design of technologies inspired by insects, such as mobile micro robots.

© 2021 Acta Materialia Inc. Published by Elsevier Ltd. All rights reserved.

1. Introduction

As the only invertebrates to evolve flight, insects interest researchers across disciplines. As a group, flying insects can hover, travel long distances, and reach speeds of 25 km per hour [1].

E-mail addresses: mark.jankauski@montana.edu (M. Jankauski), Chelsea.heveran@montana.edu (C.M. Heveran).

Most insects achieve efficiency, especially necessary for hovering, through a mechanism called indirect actuation. In indirect actuation, flight muscles deform the thorax to indirectly flap the wings [2]. The thorax has two main components- flight muscles, and the thin-walled ellipsoidal or box-like exoskeletal cuticle where flight muscles attach [2]. Cuticle is a composite of chitin, water, and proteins which is organized into distinct layers, including endocuticle, exocuticle, and epicuticle [3].

The thorax contains two main flight muscle groups, the dorsal-ventral muscles (DVM) and the dorsal-longitudinal muscles (DLM).

^{*} Corresponding authors.

Flight muscle forces are translated into flapping via intricate connections at the wing hinges [4,5]. Within the indirect lineage, fliers have either synchronous or asynchronous flight muscles. For this paper, we will distinguish these insects with asynchronous and synchronous flight muscles as asynchronous and synchronous fliers, respectively. Synchronous flight requires a neural impulse for each wing beat and is usually associated with flapping rates of <100 Hz and lineages include Lepidoptera, and higher Orthoptera [6]. Asynchronous flight has evolved independently several times and lineages include: Hymenoptera, Diptera and Coleoptera. Asynchronous flight produces work in the thorax through delayed stretch activation leading to multiple flaps per impulse [2]. Though synchronous and asynchronous muscle types are defined by the ratio of their activation frequency to the insect's wingbeat frequency, the musculature has other distinguishing characteristics as well. The stiffnesses of the two muscle groups differ greatly. Synchronous muscle is stiff when it is active and less so when passive. In asynchronous muscle, the passive muscle is stiffer than synchronous passive muscle but increases only slightly when active. The high passive stiffness in asynchronous muscle may facilitate delayed stretch activation [7]. Though there are distinct differences in stiffness between the muscle groups, it is presently unknown if there are differences between the stiffness in the cuticle that two the muscle groups attach to.

While the physiology of flight muscles has been studied extensively, the cuticle has not. In particular, the roles of thorax cuticle geometry, layering, and material gradation in flight are not well understood. Understanding cuticle heterogeneity within the thorax and between species is an essential first step for understanding the cuticle's role in efficient flight. Prior nanoindentation studies found increasing elastic modulus and hardness from the cuticle interior to exterior in the gula [8-10], infrared sensillum [9], and elytra [11] of various beetles, the grasshopper mandible [12], and the locust sternum [13]. Although many insect cuticular structures have been studied previously, the flying insect thorax has not. During flight, large cyclical forces are applied to the thorax, and thus the cuticle within the thorax might have different material constraints compared to other cuticular structure. Material gradation in other structures have been shown to provide protection and improve resilience [14,15]. A modulus gradation in the thorax would be expected to confer the same benefits, though to our knowledge, modulus gradations have not been studied in the thorax cuticle of either synchronous or asynchronous fliers.

The goal of the present work is to assess the thorax cuticle layer organization and modulus gradation for flying insects. We used histology, nanoindentation, and confocal laser scanning microscopy (CLSM) to investigate cuticle layer organization, composition (i.e., presence of resilin), and modulus gradation between distinct anatomical regions of the thorax for asynchronous (honey bee, *Apis mellifera*, *A. mellifera*) and synchronous (hawkmoth, *Manduca sexta*, *M. sexta*) fliers. We further utilized finite element analysis (FEA) to evaluate the impact of modulus gradient on thorax stress concentrations.

2. Experimental methods

2.1. Insect care and selection of regions of interest

M. sexta larvae were sourced from Josh's Frogs (Owosso, MI). Larvae were kept in inverted 0.95 liter plastic insect rearing cups (4 larvae per cup) with gutter mesh used as a climbing matrix. Rearing cups were inspected and cleaned daily. The rearing room was maintained at an ambient temperature of 28 ± 2 °C and larvae were subjected to a 24:0 (L:D) photoperiod to prevent pupal diapause [16]. Larvae were fed Repashy Superfoods Superhorn Hornworm Gutload Diet from Repashy Ventures (Oceanside, CA). Once

the dorsal aorta appeared (7–14 days), larvae were moved to a pupation chamber, a large plastic bin with a layer of damp organic potting soil and gutter screen to facilitate adult wing unfurling. Adults emerged within 14–30 days and were sacrificed within two days of emergence with ethyl acetate in a kill jar. *A. mellifera* specimens were collected from a pollinator garden in Bozeman, MT.

To determine whether thorax properties are associated with anatomy, specimens were cross-sectioned in the sagittal plane, which was selected to expose the dorsal-longitudinal flight muscles and their cuticular attachment sites (Fig. 1A). Thorax cuticle was divided into regions to better understand the cuticle variation. The *A. mellifera* thorax was divided into 4 regions (Fig. 1B): The scutum (B1), the scutellum (B2), the postscutellum (B3), and the posterior phragma (B4) [17]. The posterior phragma extends internally to provide an attachment site for the dorsal-longitudinal flight muscles. *M. sexta* was divided into 3 regions (Fig. 1C): anterior scutum where the dorsal-longitudinal muscles attach (M1), the dorsal scutum where the dorsal-ventral muscles attach (M2), and the posterior phragma, the posterior site for dorsal-longitudinal muscle attachment (M3).

2.2. Histological assessment of cuticle structure

Histological staining was used to identify variation in thoracic cuticle structure. After euthanization, specimens used in histology were preserved with 10% neutral buffered formalin overnight. Formalin fixed specimens were then dehydrated in a graded 70–100% ethanol series, embedded in paraffin, sectioned in the sagittal plane in 5 μm sections, and stained with hematoxylin and eosin (H&E) [18]. Sectioned stained cuticles were imaged with a Nikon Eclipse E800 microscope using the infinity 2 color microscope camera. White balance was set to Red = 1.33 Blue = 1.00 and Green = 2.00. To evaluate cuticle composition, five in-focus locations were selected from each region and the thickness of each cuticle layer was measured using ImageJ 1.53a.

2.3. Nanoindentation assessment of thorax cuticle modulus gradation

Separate insects than studied for histology for both species were prepared for nanoindentation analyses. Insects were dehydrated via a graded ethanol series (70–100%; at least 3 days between each step), cleared with acetone, and embedded in polymethyl methacrylate (PMMA) at 35 °C [19]. Performing nanoindentation in cross-sectioned cuticle facilitated mapping modulus gradation through the cuticle thickness while avoiding possible substrate effects that can occur from 'top down' indentation of thin structures of layers of different moduli [20,21]. The cut surface was polished with CarbiMet SiC 600 and 1000 grit abrasive paper lubricated with water, and then with progressively finer (9 to 0.05 μm ; Ted Pella) water-based alumina polishing suspension to a mirror finish. Samples were sonicated in water between polishing steps.

Nanoindentation (KLA-Tencor iMicro, Berkovich tip) was performed in load-control to a maximum load of 2 mN. The load function was 30 s ramp, 60 s hold, 10 s unload. The 60 s hold was sufficient to achieve dissipation of viscous energy, as confirmed using time-displacement plots. Non-overlapping nanoindentation arrays spanned the thorax thickness with 5 μm spacing between indents (Fig. 1D). This spacing was chosen to maximize resolution of modulus gradient throughout the cuticle while maintaining a spacing of approximately 10 times the indentation depth to minimize the impacts of the plastic zone between indents [22]. Most indents were 400–600 μm deep, which corresponds with an appropriate spacing of 8–10x the spacing between indents. About 1% of indents reached a depth of 900–1000 μm. At these depths, the depth:spacing ratio is 5–5.55, which may introduce error on

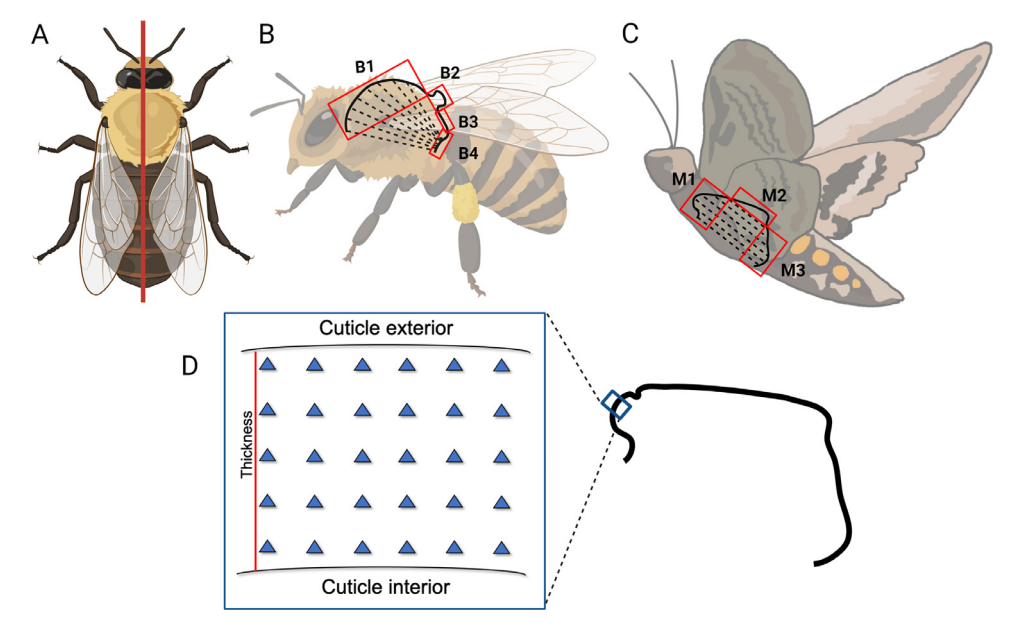


Fig. 1. Approach for thoracic cuticle assessment. (A) Insects were cross-sectioned in the sagittal plane to expose the dorsal-longitudinal muscle attachment sites and facilitate nanoindentation mapping of modulus gradation through the cuticle thickness. (B) The *A. mellifera* thorax was assigned functional regions B1–B4, where dashed lines show the dorsal-longitudinal muscles. (C) *M. sexta* was assigned functional regions M1-M3. (D) From nanoindentation data, the thickness-normalized position of each indent was calculated with reference to the cuticle interior (0 = interior, 1 = exterior).

the scale of 5–10% [22]. At least two non-overlapping arrays were placed in each thoracic region.

The reduced modulus (E_r) was calculated using the Oliver-Pharr method (Eq. (1)) [23]. A second-order polynomial was fitted to the 95th–20th percentile of the unloading portion of the load-displacement curve. Stiffness, S, was calculated as the slope of the tangent line to the start of the polynomial fit. The tip contact area (A_c) was calibrated using fused silica and measured from contact depth.

$$E_r = \frac{S}{2} \sqrt{\frac{\pi}{A_c}} \tag{1}$$

All indents were analyzed except for those that (1) were not on thorax (e.g., in plastic or on cuticle/plastic interface, determined through inspection with a 50x microscope), (2) did not demonstrate a smooth elastic-plastic transition, or (3) did not demonstrate a smooth loading-unloading curve (**Supplemental Fig. 1**). The position of each indent was calculated from the relative distance of the residual indent from the outer surface (0 = cuticle interior, 1 = cuticle exterior) (Fig. 1**D**).

2.4. Confocal laser scanning microscopy

Resilin is a rubber-like protein sometimes present in cuticle that aids in elastic energy storage. Isolated resilin has a low elastic modulus (\sim 1 MPa) that stiffens when dehydrated [3,24]. We sought to locate resilin in the thorax cuticle to identify potential areas that may have lower modulus in hydrated cuticle. Resilin

is autofluorescent, with excitation of \sim 350–407 nm and emission of \sim 413–485 nm [25]. Following nanoindentation, samples were imaged for resilin fluorescence with a Leica TCS SP5 (excitation 405 nm, emission 420–480 nm) [26]. Imaging was performed using a 25x long working distance water immersion objective. Images were processed using Imaris 9.3.0.

2.5. Finite element analysis

We developed a simple 2D FEA model (ABAQUS CAE 2019) to evaluate the impact modulus gradients had on stress in deformed cuticle (Fig. 2). The cuticle was treated as a rectangle of length 1000 µm long and height 30 µm. The height was assigned as 30 µm because this value is between the mean cuticle thickness measurements for A. mellifera (17 µm) and M. sexta (45 µm). The cuticle was discretized into 1660 linear quadrilateral S4R elements, which was sufficient for convergence of maximum stresses in all cases. For simplicity, only half the cuticle structure was modeled, where the centerline was constrained to only allow deformation along the y-axis. The lower edge has a "roller" boundary condition (represented by circles), which constrains the lower cuticle edge such that it could displace only in the x-direction. A small deformation of 5% of the cuticle thickness was prescribed in the negative y-direction at the top edge of the cuticle section. This deformation magnitude was chosen to ensure that the model remained in the geometrically linear regime. The cuticle was deformed 5% at 0 µm and the deformation linearly decreased so that the cuticle end (500 μm) was not deformed. To our knowledge, the thoracic

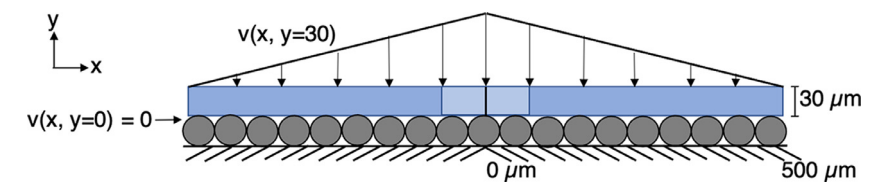


Fig. 2. FEA schematic of a 2D insect cuticle. v(x, y = 30) denotes a prescribed displacement field applied at the top edge of the cuticle w in the x-direction. We focused our discussion on middle 5% of the cuticle where the highest stress occurred (light blue). The circles at the lower edge represent a "roller" boundary condition, where the bottom edge of the cuticle is constrained so that it cannot displace in the y-direction but can displace in the x-direction.

cuticle deformation (which is not identical to bulk thorax deformation) during flight has not been measured in any insect. Stress depends on material properties as well as thorax geometry. By choosing modulus and cuticle thickness values that are representative of experimental values for *A. mellifera* and *M. sexta*, we gain a qualitative understanding of how modulus gradients affect stress accumulation in insect cuticle.

For the material, we assigned a Poisson's ratio of 0.3 and one of two elastic moduli distributions. The first was a single uniform modulus of 7 GPa, and the second was a 2 GPa linear gradient in the y-direction with a mean modulus of 7 GPa. We considered a positive modulus gradient to represent forces that may be applied from the exterior such as during predation or burrowing. We also considered a model with a negative modulus gradient to represent forces that may be acting from the interior such as flight muscles. In all cases the cuticle material was assumed linear-elastic and isotropic. We focused on the area with the largest stress values by zooming in on the 5% of the cuticle with the largest imposed displacement. Results were mirrored to show the effect of deformation in both directions.

2.6. Statistics

For nanoindentation, two specimens for each species were studied. Between 2 and 7 arrays were collected for each region. To avoid oversampling some regions, two arrays were randomly se-

lected from each region for each specimen for analysis. We sought to test the hypotheses that (1) mean modulus and (2) modulus gradation through the cuticle thickness vary by region. To test our first hypothesis, we generated a mixed model ANOVA with the random effects of specimen and array and the fixed effect of region. To test our second hypothesis, we used a linear mixed model with random effects of specimen and array, fixed effect of region, and a covariate of indent relative position. Relative positions were assigned within the thorax thickness, where 0 indicates the cuticle interior and 1 indicates the cuticle exterior. Separate models were generated for each insect species. For histology, three specimens for each species were evaluated. Mixed model ANOVA (random effect of specimen, fixed effect of region) for each insect species tested the effect of region on cuticle thickness and the composition of layers. Modulus was squared or log transformed, when necessary, to satisfy ANOVA assumptions of residual normality and homoscedasticity. All statistical tests were performed using Minitab v. 19 2020 2.0. The threshold for significance was set a priori at p < 0.05 for all tests.

3. Results

3.1. Histology

H&E staining showed that the thorax composition is heterogeneous between regions for A. mellifera and M. sexta (Fig. 3). All A.

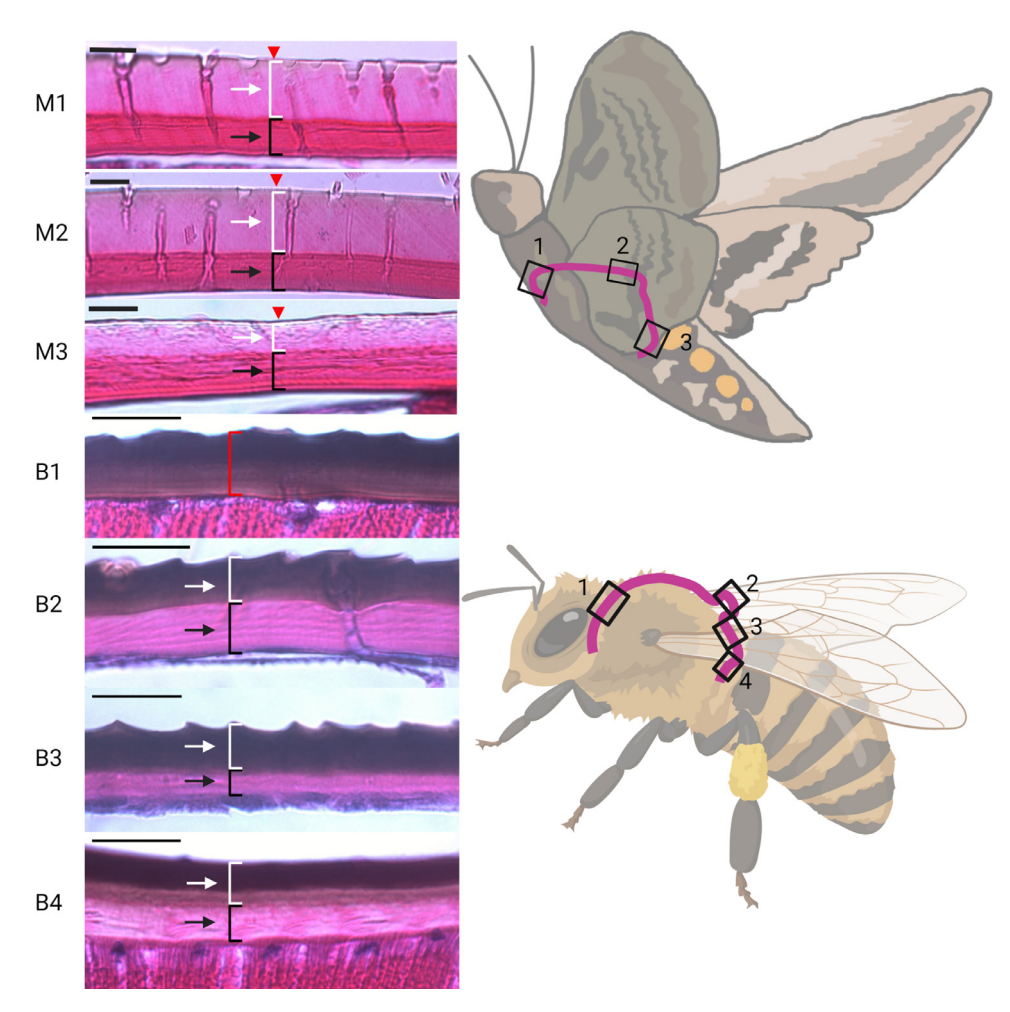


Fig. 3. Thorax structure from H&E-stained sections differs by insect and region. For all images, the cuticle interior is on the bottom. Endocuticle (black arrows) and exocuticle (white arrows) thicknesses vary between thorax regions for *A. mellifera* and *M. sexta*. An epicuticle (red arrows) was only observed for *M. sexta*. *A. mellifera* and *M. sexta* cuticle samples were imaged at 60x and 20x, respectively. Scale bars: 20 μm.

Table 1Cuticle layer composition by region for A. mellifera (B1-B4) and M. sexta (M1-M3). Thickness and percentages (with respect to the total thickness) are reported as mean \pm standard deviation.

Cuticle Layer	B1	B2	В3	B4	M1	M2	M3
Total (µm)	16 ± 0.40	24 ± 0.73	13 ± 2.5	18 ± 7.8	49 ± 2.8	45 ± 3.6	30 ± 4.3
Epicuticle	_	-	_	-	$2.8\pm0.55~\mu m$	$4.2\pm1.9~\mu m$	$2.4\pm0.36~\mu m$
					$6.2\pm1.3\%$	$10\pm5.3\%$	$7.9\pm0.24\%$
Exocuticle	=	$9.2\pm0.52~\mu m$	$6.3\pm1.3~\mu m$	$7.3\pm2.3~\mu m$	21 \pm 3.3 μm	$19\pm5.0~\mu m$	$13 \pm 3.4 \ \mu m$
		$39\pm2.6\%$	$50\pm4.4\%$	$41\pm6.7\%$	$43\pm5.2\%$	$42\pm8.9\%$	$48\pm3.6\%$
Endocuticle	_	$15\pm0.83\;\mu m$	$6.5\pm1.5~\mu m$	$11 \pm 5.5 \ \mu m$	$25\pm2.2\;\mu m$	$24\pm2.0\;\mu m$	$14\pm1.4~\mu m$
		$61~\pm~2.6\%$	$50\pm4.4\%$	$59\pm6.7\%$	$51\pm6.5\%$	$53\pm4.4\%$	$55 \pm 15\%$

mellifera regions had distinct exocuticle and endocuticle (noted by the stark difference in pink color) except for region B1, where these layers were not distinct. *M. sexta* had distinct endocuticle and exocuticle separation for most of the thorax, but occasionally these layers were not distinct in M3. *M. sexta* epicuticle is visible as a thin dark line on the cuticle exterior, which is not seen in *A. mellifera*. The epicuticle may not be visible with the dark staining of the exocuticle. *A. mellifera* exocuticle showed dark exocuticle staining for all regions.

For each insect, the thorax composition for each region is reported in Table 1. For A. mellifera, region did not have a significant effect on total cuticle thickness (p > 0.05). Endocuticle thickness (µm) did vary by region (p = 0.038), with B3 being 56% thinner than B2 (p = 0.047) and B4 not being significantly different than either B2 and B3. Exocuticle thickness did not vary by region. Epicuticle was not detected for A. mellifera. Relative cuticle composition (% of cuticle thickness by layer) did not significantly vary by region. We note that cuticle layering was more difficult to measure in B1, where layers were not distinct. For M. sexta, there was a significant effect of region on total cuticle thickness (p < 0.001). M1 and M2 had similar thicknesses while M3 was significantly thinner than M1 (p < 0.001) and M2 (p = 0.002). Endocuticle also depended on region (p < 0.001). The endocuticle for M3 was significantly thinner than for M1 (p < 0.001) and M2 (p = 0.002). Exocuticle and epicuticle thickness did not differ by region (p > 0.05). The relative composition of cuticle did not vary by region. Some measurements in M3 did not show a clear distinction of endocuticle and exocuticle and in these cases only the total and epicuticle thickness were calculated.

3.2. Nanoindentation and CLSM

We used nanoindentation to evaluate the dependence of mean cuticle modulus and modulus gradation on thorax region. The mean modulus did not differ between region for either *A. mellifera* or *M. sexta* (p > 0.05 for both). When all data were averaged between regions, modulus did not differ between *A. mellifera* (7.11 ± 1.47 GPa) and *M. sexta* (6.75 ± 1.92 GPa) (p > 0.05).

Nanoindentation modulus was graded with respect to cuticle position for *A. mellifera* (Fig. 4). This gradation was approximately linear, increasing from the cuticle interior (relative position = 0) to the exterior (relative position = 1) (**Supplemental Fig. 2**). We used mixed model ANOVA to evaluate whether these gradations differed between regions for *A. mellifera*. There was a significant (p < 0.001) interaction between region and relative position, indicating that the linear gradient of modulus (i.e., slope) differs between regions. Eq. (2) describes the marginal fits for E_r (GPa) by region for *A. mellifera* from mixed model ANOVA.

B1 :
$$E_r = 6.73 + 0.797 * \text{relative position}$$

B2 : $E_r = 5.58 + 3.07 * \text{relative position}$
B3 : $E_r = 4.96 + 2.00 * \text{relative position}$
B4 : $E_r = 6.04 + 3.12 * \text{relative position}$

The slope in B1 was close to 0 and was much less (97–118%) than in B2-B4. While a single estimate of slope represented most

of *A. mellifera* regions well (Fig. 4), B4 was more variable. Half of the arrays in this region had a steep positive slope and half had a slight negative slope which resulted in a mean positive slope. Modulus gradients for *M. sexta* were variable in both direction and shape with no single approximation appropriate for the regional representation of the data. The four arrays from each region that were included in the ANOVA and in Fig. 4 were randomly selected from a larger sample size which showed similar trends (**Supplemental Fig. 3**).

Because dehydrated resilin stiffen the cuticle [24,25], we employed CLSM to identify areas of cuticle that have the potential for low elastic modulus in hydrated cuticle due to resilin. Resilin identified from blue autofluorescence was present in the cuticle of both insects but varied by species and thorax region (**Supplemental Figs. 4 and 5**). The presence of resilin was not associated with a particular modulus value (high or low modulus), including regions where resilin was present only on either the cuticle interior or exterior (Fig. 4, **Supplemental Figs. 4 and 5**).

3.3. Finite element analysis

FEA was used to investigate how experimentally-observed modulus gradients influenced stress distributions in the deformed *A. mellifera* cuticle. *M. sexta* modulus distribution varied so much within each region that modeling a particular gradation would not be generalizable. A homogenous cuticle was first modeled to provide a baseline calculation of stress distribution. The cuticle was assigned a modulus of 7 GPa from the mean experimental data. A second model considered elastic moduli that varied linearly from 6 to 8 GPa through the cuticle thickness. A slope of 2 GPa increase across the cuticle thickness was chosen based on an average estimate of slope for *A. mellifera*. The slope was applied in the positive y-direction and, in a separate model, the negative y-direction based on the potential for forces from flight muscles or from external sources to be acting on the cuticle.

The linear modulus gradient influenced the maximum stress, but the stress distribution was insensitive to modulus gradient or direction (Fig. 5). When the deformation was applied to the high modulus edge, the linearly-graded cuticle experienced a maximum stress 15.3% less than the homogenous cuticle. On the other hand, when the deformation was applied to the low modulus edge, the linearly-graded cuticle experienced a maximum stress 13.3% greater than that experienced by the homogeneous cuticle. This complexifies the stress reduction in the thorax cuticle. Based on our simplified FEA model, a linearly distributed modulus cannot optimally reduce stress for both interior deformation due to flight muscles and exterior deformation from external forces.

4. Discussion

The thorax is essential for insect flight, yet significant questions remain about its mechanical properties. The thorax must be flexible enough to articulate the wing but must also protect against external forces and resist plastic deformation under the high mag-

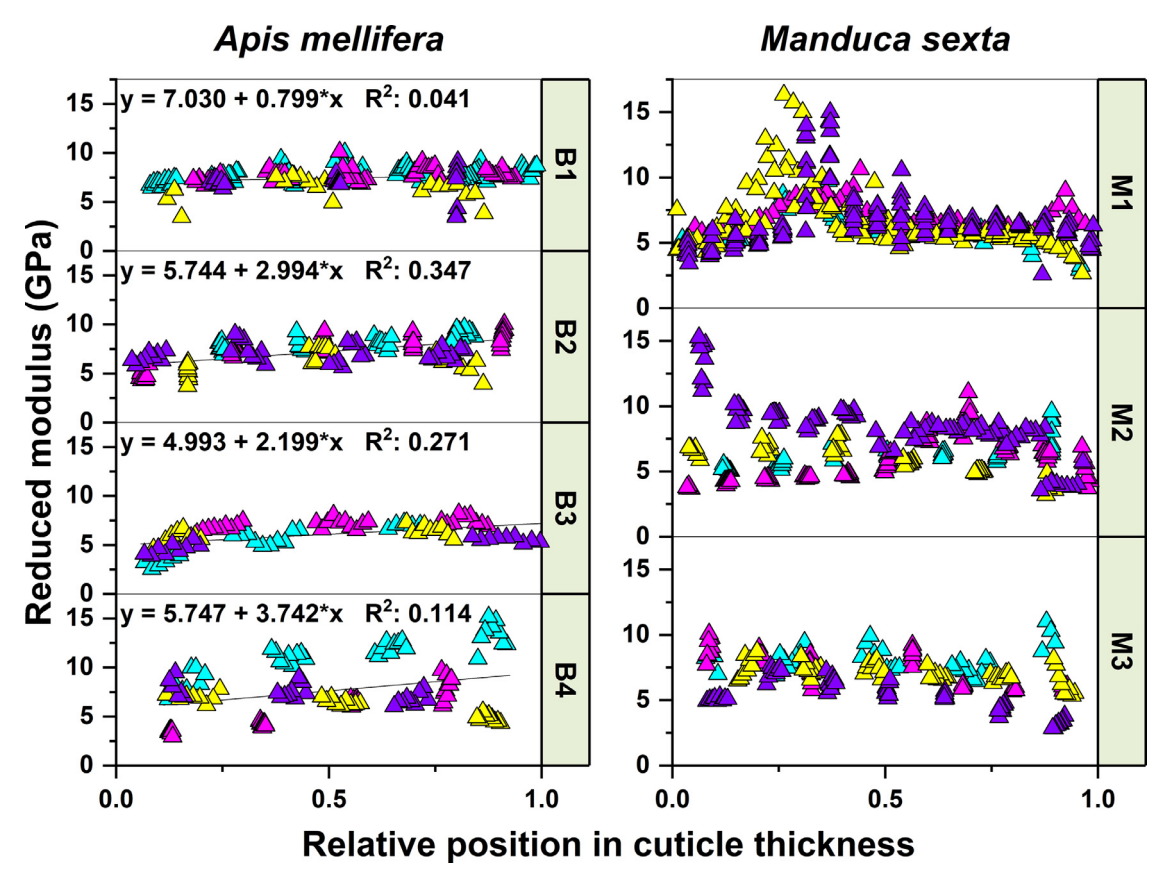


Fig. 4. Modulus gradation through the cuticle thickness where 0 indicates cuticle interior and 1 indicates exterior. Data are those analyzed for *A. mellifera* and *M. sexta*. Each color represents all indents from one array per region. *A. mellifera* modulus gradients were well-represented by linear fits for all regions. Modulus did not show consistent gradation for *M. sexta* in any region.

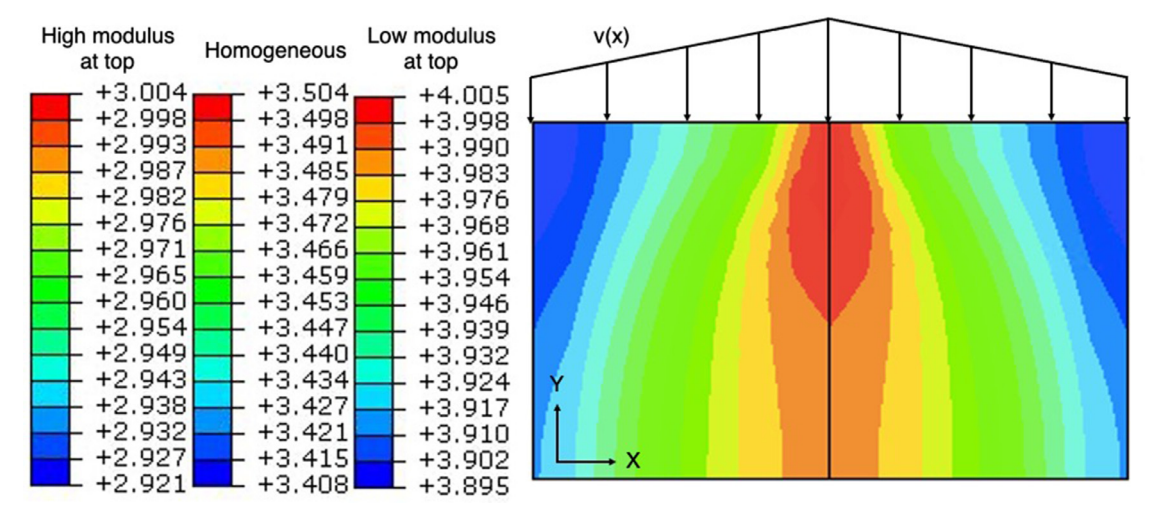


Fig. 5. Stress distribution (10⁸ Pa) from a 5% deformation of 2D thoracic cuticle models. The lowest stress accumulation occurred when the higher modulus edge of the linear distribution was deformed.

nitude forces produced by the flight muscles. Furthermore, the thorax stores and releases elastic energy over a large number of oscillations (e.g., 10⁷ oscillations for *A. mellifera* [27]) without fatigue. Modulus gradients are observed in other biological materials (e.g., enamel, bamboo, elastomeric fibers) where they help maintain a balance of strength, resilience, and toughness and minimize stress concentrations in complex geometrical structures [28–31]. The purposes of this study were to determine whether insect thorax has graded moduli through the cuticle thickness, whether these gradients depend on thorax region and species, and whether the

ulus gradients impact thorax stress concentrations. Understanding thorax cuticle material variation is a necessary step in determining its roles in insect flight.

We performed nanoindentation on ethanol-dehydrated, plastic-embedded samples of thorax cuticle. The mean moduli for thorax cuticle in both *A. mellifera* and *M. sexta* were in good agreement with values reported for different insect structures. Our measurement of \sim 7 GPa for dehydrated thorax cuticle for *A. mellifera* and *M. sexta* is within the 4.8 to 9.9 GPa reported for the beetle gula [8–10], elytra [11,32], and infrared sensillum [9], and the locust

sternum [13] and tibia [33]. These are among the first nanoindentation evaluations for the flying insect thorax cuticle, and specifically within the *Hymenoptera* and *Lepidoptera* taxa [34,35]. Studies comparing nanoindentation results from dried and fresh cuticle of the beetle gula [8,10], locust sternum [13], and termite mandibles [36] showed modulus increases of 10% to upwards of 500% with dehydration. Our thorax moduli for *M. sexta* were \sim 25% greater than for modulus values of the fresh thorax reported for the same species [35]. This level of stiffening from dehydration is on par with that observed in bone embedded in PMMA [19]. We find this to be an acceptable tradeoff for high spatial resolution testing which is difficult to achieve in fresh samples because of higher surface roughness.

Modulus varied throughout the thorax thickness, but the direction and steepness of this gradient depended on insect and region. For two of the four regions, A. mellifera had steep, positive, linear, modulus gradients from cuticle interior to exterior. The positive modulus gradient in A. mellifera thorax agrees with gradients found in non-thorax cuticle for some other insects. Previous work demonstrates that the modulus increases from the cuticle interior to exterior for the gula [8-10], infrared sensillum [9], and elytra [11] of various beetles, the grasshopper mandible [12], and the locust sternum [13]. Increased modulus is observed with sclerotization [37,38], including for some of these insect structures [9,33]. Sclerotization is also associated with dark staining in H&E histology [39,40]. For A. mellifera, the dark staining at the thorax exterior from histological sections indicates that higher modulus is also likely to be influenced by sclerotization. A similar dark staining is seen for Drosophila melanogaster abdomen cuticle [41]. However, sclerotization cannot be the only contributor to modulus gradation, since dark banding was seen on the exterior of all A. mellifera histological sections but did not always align with the higher modulus seen at the exterior of the same regions. The apparent lack of sclerotization in the cuticle for M. sexta may partially explain the differences in modulus gradation between M. sexta and A. mellifera found in this study. The differences between A. mellifera and M. sexta thorax cuticle may also be adaptations for behaviors separate from or in conjuncture with flight. For example, most cases of increasing modulus gradient, as seen in A. mellifera, are found for cuticle optimized for protection against predation or during burrowing [11,15,42]. Although A. mellifera do not burrow, most Hymenoptera do (e.g., genera Xylocopa, Andrenida [43]). Thus, the protective cuticle may be residual in the Hymenoptera lineage to adapt for burrowing.

We used FEA to assess the impact of the modulus gradient found in A. mellifera on cuticle stress concentration. The 2 GPa gradient applied in FEA may vary from the exact gradient observed in living insect cuticle because the analysis includes data from dehydrated samples, but assuming the stress is in the linear regime, there is a linear relationship between the modulus slope and the stress concentrations. Lower stress accumulation is essential for avoiding permanent deformations that could impact thorax performance. The cuticle accumulated the least stress when its modulus was distributed linearly through the thickness, and it was compressed from the highest modulus side. For A. mellifera, this type of compression would likely result from external forces, which fits with our hypothesis that the cuticle gradient is optimized for protection. While simplified, these models illustrate that graded moduli distribution can reduce stress accumulation in some loading contexts. However, further work needs to be done to understand how bulk thorax geometry coupled with cuticle material variation influence peak stresses and energy storage during flight.

The thorax likely uses several mechanisms to increase energy return during flight. For both synchronous (e.g., *M. sexta*) and asynchronous (e.g., *A. mellifera*) fliers, large power requirements, and low muscular efficiency (<10%) necessitate energy storage in the

thorax [44]. Passive, asynchronous muscle is stiffer and behaves more spring-like relative to synchronous muscle [7]. This passive stiffness may be one way that asynchronous muscle stores elastic energy. In *M. sexta*, mechanical coupling of the scutum and the wing hinges is believed to increase energy return by decoupling the area where the most power is lost (wing hinges) and where the most energy is returned (scutum) [45,46]. Our results suggest that cuticle stiffness does not differ between flying insect lineages, but that the material gradient does. Material gradients may also play a role in this elastic energy storage. Modulus gradients can increase energy return in biomaterials and bioinspired polymers by increasing stretching [30,31]. Further research is needed to identify how these properties or others adapt the thorax cuticle for energy storage in different flight lineages.

While this study has elucidated the material properties and structure of flight insect thorax cuticle, the main limitation to our approach is the effect of dehydration. Dehydrating the cuticle was necessary to achieve high spatial resolution for nanoindentation. However, dehydration may stiffen the cuticle non-uniformly, and thus material gradients measured in dehydrated samples may not represent the in vivo material gradients. For instance, it is possible that cuticle with high resilin concentration stiffens more than other areas of cuticle with dehydration, in which case the in vivo gradation would not be observed in our dehydrated samples. Prior literature shows that the effects of dehydration on cuticle material property gradation are inconsistent. Modulus gradients have been shown to disappear and sometimes reverse in dehydrated samples [13,47], though other studies have shown hydrated and dehydrated cuticle demonstrate similar modulus gradients in two species of beetle gula [8,10]. Thus, it is not possible to generalize how dehydration changes our observed gradations from the in vivo state.

5. Conclusions

We demonstrate that the flying insect thorax is heterogeneous with respect to structure, material composition, and modulus gradient. In *A. mellifera*, a clear linear modulus gradation is observed in two of the four anatomic regions of interest within the thorax. This linear gradient of modulus with thorax thickness may contribute to decreased stress concentration and protection. This work investigating the properties of the thorax cuticle is a crucial first step for determining the relative contributions of cuticle structure, material composition, and modulus gradient to the efficiency of different forms of flight.

Funding statement

This research was partially supported the National Science Foundation under awards No. CMMI-1942810 to MJ. Any opinions, findings, and conclusions or recommendations expressed in this material are those of the author(s) and do not necessarily reflect the views of the National Science Foundation.

Declaration of Competing Interest

The authors declare that they have no known competing financial interests or personal relationships that could have appeared to influence the work reported in this paper.

CRediT authorship contribution statement

Cailin Casey: Conceptualization, Data curation, Formal analysis, Writing – original draft, Writing – review & editing. **Claire Yager:** Conceptualization, Writing – review & editing. **Mark Jankauski:** Conceptualization, Funding acquisition, Writing – original draft,

Writing – review & editing. **Chelsea M. Heveran:** Conceptualization, Formal analysis, Writing – original draft, Writing – review & editing.

Acknowledgments

We would like to thank Dr. Robert KD Peterson and Miles Maxcer for helping raise insects and Ghazal Vahidi for assistance in sample preparation for nanoindentation.

Supplementary materials

Supplementary material associated with this article can be found, in the online version, at doi:10.1016/j.actbio.2021.10.035.

References

- [1] A. Azuma, T. Watanabe, Flight performance of a dragonfly, J. Exp. Biol. 137 (1988) 221–252.
- [2] J.W.S. Pringle, The excitation and contraction of the flight muscles of insects, J. Physiol. 108 (1949) (Lond.), doi:10.1113/jphysiol.1949.sp004326.
- [3] J.F.V. Vincent, U.G.K. Wegst, Design and mechanical properties of insect cuticle, Arthropod Struct. Dev. 33 (2004) 187–199, doi:10.1016/j.asd.2004.05.006.
- [4] W. Nachtigall, A. Wisser, D. Eisinger, Flight of the honey bee. VIII. Functional elements and mechanics of the "flight motor" and the wing joint-one of the most complicated gear-mechanisms in the animal kingdom, J. Comp. Physiol. B 168 (1998) 323-344.
- [5] M.B. Rheuben, A.E. Kammer, Structure and innervation of the third axillary muscle of Manduca relative to its role in turning flight, J. Exp. Biol. 131 (1987) 373–402.
- [6] O.W. Tiegs, The flight muscles of insects-their anatomy and histology; with some observations on the structure of striated muscle in general, Philos. Trans. R. Soc. Lond. B Biol. Sci. 238 (1955) 221–348.
- [7] R.K. Josephson, J.G. Malamud, D.R. Stokes, Asynchronous muscle: a primer, J. Exp. Biol. 203 (2000) 2713–2722.
- [8] N. Barbakadze, S. Enders, S. Gorb, E. Arzt, Local mechanical properties of the head articulation cuticle in the beetle Pachnoda marginata (Coleoptera, Scarabaeidae), J. Exp. Biol. 209 (2006) 722–730, doi:10.1242/jeb.02065.
- [9] M. Müller, M. Olek, M. Giersig, H. Schmitz, Micromechanical properties of consecutive layers in specialized insect cuticle: the gula of Pachnoda marginata (Coleoptera, Scarabaeidae) and the infrared sensilla of Melanophila acuminata (Coleoptera, Buprestidae), J. Exp. Biol. 211 (2008) 2576–2583, doi:10.1242/jeb. 020164
- [10] S. Enders, N. Barbakadse, S.N. Gorb, E. Arzt, Exploring biological surfaces by nanoindentation, J. Mater. Res. 19 (2004) 880–887, doi:10.1557/jmr.2004.19.3. 880.
- [11] J.Y. Sun, J. Tong, J. Zhou, Application of nano-indenter for investigation of the properties of the elytra cuticle of the dung beetle (Copris ochus Motschulsky), IEE Proc. Nanobiotechnol. 153 (2006) 129–133, doi:10.1049/ip-nbt:20050050.
- [12] T. Schöberl, I.L. Jäger, Wet or dry hardness, stiffness and wear resistance of biological materials on the micron scale, Adv. Eng. Mater. 8 (2006) 1164–1169, doi:10.1002/adem.200600143.
- [13] D. Klocke, H. Schmitz, Water as a major modulator of the mechanical properties of insect cuticle, Acta Biomater. 7 (2011) 2935–2942, doi:10.1016/j.actbio. 2011.04.004.
- [14] H. Rajabi, M. Jafarpour, A. Darvizeh, J.H. Dirks, S.N. Gorb, Stiffness distribution in insect cuticle: a continuous or a discontinuous profile? J. R. Soc. Interface 14 (2017), doi:10.1098/rsif.2017.0310.
- [15] M. Jafarpour, S. Eshghi, A. Darvizeh, S. Gorb, H. Rajabi, Functional significance of graded properties of insect cuticle supported by an evolutionary analysis: functional significance of graded properties of insect cuticle supported by an evolutionary analysis, J. R. Soc. Interface 17 (2020), doi:10.1098/rsif.2020. 0378rsif20200378.
- [16] R.A. Bell, C.G. Rasul, F.G. Joachim, Photoperiodic induction of the pupal diapause in the tobacco hornworm, Manduca sexta, J. Insect Physiol. 21 (1975) 1471–1480.
- [17] R.E. Snodgrass, The thorax of the hymenoptera, US Government Printing Office, 1910.
- [18] A.J. Clark, J.D. Triblehorn, Mechanical properties of the cuticles of three cockroach species that differ in their wind-evoked escape behavior, PeerJ 2 (2014) e501.

- [19] A.J. Bushby, V.L. Ferguson, A. Boyde, Nanoindentation of bone: comparison of specimens tested in liquid and embedded in polymethylmethacrylate, J. Mater. Res. 19 (2004) 249–259.
- [20] X. Chen, J.J. Vlassak, Numerical study on the measurement of thin film mechanical properties by means of nanoindentation, J. Mater. Res. 16 (2001) 2974–2982.
- [21] Y.G. Jung, B.R. Lawn, M. Martyniuk, H. Huang, X.Z. Hu, Evaluation of elastic modulus and hardness of thin films by nanoindentation, J. Mater. Res. 19 (2004) 3076–3080.
- [22] P. Sudharshan Phani, W.C. Oliver, A critical assessment of the effect of indentation spacing on the measurement of hardness and modulus using instrumented indentation testing, Mater. Des. 164 (2019), doi:10.1016/j.matdes.2018. 107563
- [23] W.C. Oliver, G.M. Pharr, An improved technique for determining hardness and elastic modulus using load and displacement sensing indentation experiments, J. Mater. Res. 7 (1992) 1564–1583.
- [24] T. Weis-Fogh, Thermodynamic properties of resilin, a rubber-like protein, J. Mol. Biol. 3 (1961) 520–531.
- [25] M. Burrows, S.R. Shaw, G.P. Sutton, Resilin and chitinous cuticle form a composite structure for energy storage in jumping by froghopper insects, BMC Biol. 6 (2008) 1–16, doi:10.1186/1741-7007-6-41.
- [26] J. Michels, S.N. Gorb, Detailed three-dimensional visualization of resilin in the exoskeleton of arthropods using confocal laser scanning microscopy, J. Microsc. 245 (2012) 1–16, doi:10.1111/j.1365-2818.2011.03523.x.
- [27] P.K. Visscher, R. Dukas, Survivorship of foraging honey bees Insectes Sociaux, 1997.
- [28] A.R. Studart, Biological and bioinspired composites with spatially tunable heterogeneous architectures, Adv. Funct. Mater. 23 (2013) 4423–4436.
- [29] S. Amada, Y. Ichikawa, T. Munekata, Y. Nagase, H. Shimizu, Fiber texture and mechanical graded structure of bamboo, Compos. Part B Eng. 28 (1997) 13–20.
- [30] J.H. Waite, E. Vaccaro, C. Sun, J.M. Lucas, Elastomeric gradients: a hedge against stress concentration in marine holdfasts? Philos. Trans. R. Soc. Lond. Ser. B Biol. Sci. 357 (2002) 143–153.
- [31] Z. Wu, S. Zhang, A. Vorobyev, K. Gamstedt, K. Wu, C. Guo, S.H. Jeong, Seamless modulus gradient structures for highly resilient, stretchable system integration, Mater. Today Phys. 4 (2018) 28–35.
- [32] Z. Dai, Z. Yang, Macro-/micro-structures of elytra, mechanical properties of the biomaterial and the coupling strength between elytra in beetles, J. Bionic Eng. 7 (2010) 6–12, doi:10.1016/S1672-6529(09)60187-6.
- [33] C. Li, S.N. Gorb, H. Rajabi, Cuticle sclerotization determines the difference between the elastic moduli of locust tibiae, Acta Biomater. 103 (2020) 189–195, doi:10.1016/j.actbio.2019.12.013.
- [34] K. Stamm, B.D. Saltin, J.H. Dirks, Biomechanics of insect cuticle: an interdisciplinary experimental challenge, Appl. Phys. A 127 (2021) 1–9.
- [35] A.C. Hollenbeck, A.N. Palazotto, Mechanical characterization of flight mechanism in the hawkmoth Manduca sexta, Exp. Mech. 53 (2013) 1189–1199, doi:10.1007/s11340-013-9726-5.
- [36] B.W. Cribb, A. Stewart, H. Huang, R. Truss, B. Noller, R. Rasch, M.P. Zalucki, Insect mandibles comparative mechanical properties and links with metal incorporation, Naturwissenschaften 95 (2008) 17–23, doi:10.1007/s00114-007-0288-1.
- [37] S.O. Andersen, Insect cuticular sclerotization: a review, Insect Biochem. Mol. Biol. 40 (2010) 166–178.
- [38] J.F. Vincent, Insect cuticle: a paradigm for natural composites, Symp. Soc. Exp. Biol. 34 (1980) 183–210.
- [39] F. Stringfellow, Functional morphology and histochemistry of structural proteins of the genital cone of Cooperia punctata (von Linstow, 1907) Ransom, 1907, a nematode parasite of ruminants, J. Parasitol. (1969) 1191–1200.
- [40] S.O. Andersen, M.G. Peter, P. Roepstorff, Cuticular sclerotization in insects, Comp. Biochem. Physiol. B Biochem. Mol. Biol. 113 (1996) 689–705.
- 41] T. Sztal, H. Chung, S. Berger, P.D. Currie, P. Batterham, P.J. Daborn, A cytochrome p450 conserved in insects is involved in cuticle formation, PLoS One 7 (2012) e36544.
- [42] Y. Xing, J. Yang, Stiffness distribution in natural insect cuticle reveals an impact resistance strategy, J. Biomech. 109 (2020) 109952, doi:10.1016/j.jbiomech. 2020.109952.
- [43] S.W.T. Batra, Solitary bees, Sci. Am. 250 (1984) 120–127.
- [44] C.P. Ellington, Power and efficiency of insect flight muscle, 1985.
- [45] J. Gau, N. Gravish, S. Sponberg, Indirect actuation reduces flight power requirements in Manduca sexta via elastic energy exchange, J. R. Soc. Interface 16 (2019) 1–17, doi:10.1098/rsif.2019.0543.
- [46] N. Ando, R. Kanzaki, Flexibility and control of thorax deformation during hawkmoth flight, Biol. Lett. 12 (2016), doi:10.1098/rsbl.2015.0733.
- [47] H. Peisker, J. Michels, S.N. Gorb, Evidence for a material gradient in the adhesive tarsal setae of the ladybird beetle Coccinella septempunctata, Nat. Commun. 4 (2013) 1–7, doi:10.1038/ncomms2576.